Spectral Evolution in $(Ca,Sr)RuO_3$ near the Mott-Hubbard Transition

J. S. Ahn,[1] J. Bak,[1] H. S. Choi,[1] T. W. Noh,[1] J. E. Han,[2] Yunkyu Bang,[3] J. H. Cho,[4] and Q. X. Jia[5]
[1]*Department of Physics, Seoul National University, Seoul 151-742, Korea*
[2]*Max-Planck Institut für Festkörperforschung, Heisenbergstrasse 1, D-70569, Stuttgart, Germany*
[3]*Department of Physics, Chonnam National University, Kwangju 500-757, Korea*
[4]*RCDAMP and Department of Physics, Pusan National University, Pusan 609-735, Korea*
[5]*Superconductivity Technology Center, Los Alamos National Laboratory, Los Alamos, New Mexico 87545*
(Received 14 July 1998)

We investigated optical properties of $(Ca,Sr)RuO_3$ films on the borderline of a metal-insulator transition. Our results show all of the predicted characteristics for a metallic Mott-Hubbard system, including (i) a mass enhancement in dc limit, (ii) a $U/2$ excitation, and (iii) a U excitation. Also, self-consistency is exploited within the Gutzwiller-Brinkman-Rice picture for the Mott transition. Our finding displays that electron correlation should be important even in $4d$ materials. However, low frequency behaviors of electrodynamic quantities suggest extra scattering mechanisms in addition to the Mott-Hubbard correlation. [S0031-9007(99)09525-3]

PACS numbers: 71.30.+h, 71.10.Fd, 71.27.+a, 78.20.–e

A metal-insulator (M-I) transition driven by electron correlation was proposed by Mott and subsequently investigated intensively [1]. Since the Hubbard model was proposed, it has been widely accepted as the simplest model which can describe correlation effects. Although the model is composed of only two parameters, i.e., intersite hopping energy t $(= W/z)$ and on-site Coulomb repulsive energy U, it has not been exactly solved yet except for the one dimensional case. (W and z are the bandwidth and the coordination number, respectively.) Until several years ago, different approaches provided limited insight into different aspects of the M-I transition. However, recent theoretical progress, including a slave-boson approach, infinite dimension limit approaches with several techniques, and numerical calculations for finite size systems, started to provide a coherent picture [2].

According to the traditional Gutzwiller-Brinkman-Rice (GBR) picture [3], the Mott M-I transition from a metallic side can be described by the narrowing and the disappearing of a Fermi liquid quasiparticle (QP) band at a critical value of correlation strength, $(U/W)_c$. Under this strong renormalization, an effective mass, m^* [4], of the QP is related by

$$\frac{1}{m^*} = 1 - \frac{(U/W)^2}{(U/W)_c^2}. \qquad (1)$$

Recent results from the dynamical mean field theory (DMFT) predict that one particle spectral function $A(\omega)$ for the *metallic side* will be split into lower (LHB) and upper (UHB) Hubbard bands, in addition to the QP band located at zero frequency [2]. Figure 1(a) shows the schematic diagram of $A(\omega)$. Then, the corresponding optical conductivity spectra $\sigma_1(\omega)$ can be easily predicted and displayed in Fig. 1(b). Note that $\sigma_1(\omega)$ in a metallic side has three pronounced features: (i) a "QP peak" near zero frequency, (ii) a "$U/2$ peak" due to optical transitions between QP band and LHB (or UHB), and (iii) a "U peak" due to a transition between LHB and UHB.

Most experimental efforts to investigate the Mott M-I transition have been focused on $3d$ metal oxides. $LaTiO_3$ and $LaVO_3$ have been considered as prototypes of Mott insulators [5]. One way of inducing the M-I transition is to dope the compounds with carriers, which changes the band filling. Optical properties of such band-filling controlled compounds show mass enhancements and spectral weight changes [6]. Another way is to substitute the rare earth element, which changes the bandwidth. For the bandwidth controlled compounds in the insulating side, such as $(La,Y)TiO_3$, a systematic gap change was observed with the substitution. Values of $(U/W)_c$ for $(La,Y)TiO_3$ were estimated to be about 1.6 [7]. Recently, Rozenberg *et al.* showed that $(Ca,Sr)VO_3$ could be treated as a bandwidth controlled compound in the metallic side [8]. The optical properties of $(Ca,Sr)VO_3$ showed the predicted $\sigma_1(\omega)$ features due to correlation, shown in Fig. 1, in line with the DMFT approach starting from V_2O_3 [9]: however, the critical mass enhancement was not observed [10,11]. Therefore, as far as we know, there are no optical data which simultaneously display the predicted behaviors of $\sigma_1(\omega)$ and $1/m^*$ in the metallic side.

In this Letter, we report optical properties of $(Ca,Sr)RuO_3$ films, where four $4d$ electrons occupy triple degenerate t_{2g} levels. Generally speaking, correlation effects are believed to be less important in describing

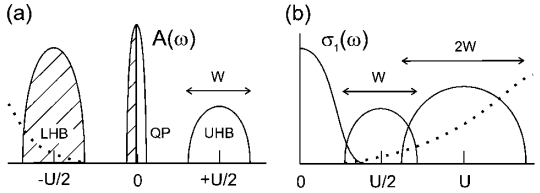

FIG. 1. Schematic diagrams of (a) one particle spectral function and (b) optical conductivity, for the 4/6 filled metallic Mott-Hubbard system. Dotted lines indicate the contributions from the O($2p$) band.

$4d$ electrons than $3d$ ones, because the less localized the electron wave function is, the weaker the correlation effects are. However, recent works on layered perovskite ruthenates showed that the correlation effect might play an important role in determining their physical properties [12–16]. A recent far-infrared study on perovskite $SrRuO_3$ films indicated that their responses might differ from the predictions of Fermi liquid [17]. Therefore, we will critically review our results in the light of the correlation effect.

$SrRuO_3$ is known to be a bad metal which shows a ferromagnetic ordering at $T_c \sim 160$ K. $CaRuO_3$ is also barely metallic, but it does not show any magnetic ordering down to 4.2 K. Photoemission data showed that $CaRuO_3$ has a narrower bandwidth than $SrRuO_3$, so that it stands on the borderline of *M-I* transitions in ternary Ru^{4+} oxides [18]. Therefore, if epitaxial $CaRuO_3$ thin films are fabricated, their electrical properties can be easily controlled from metal to insulator through the strain effect [19]. Using this effect, we were able to prepare epitaxial (Ca,Sr)RuO_3 thin films, where the Ca substitution makes them closer to the *M-I* transition.

(Ca,Sr)RuO_3 films were grown on single crystal $SrTiO_3$(100) substrates by pulsed laser deposition [20]. Figure 2 shows the temperature dependent dc resistivity ρ_{dc} curves. The $SrRuO_3$ film shows a metallic behavior with a small slope change around 140 K, which corresponds to its T_c value. Both of the $Ca_{0.5}Sr_{0.5}RuO_3$ and the $CaRuO_3$ films show barely metallic behaviors: their ρ_{dc} values are close to about 1000 $\mu\Omega$ cm, which corresponds to the Mott minimum metallic conductivity [1]. The ρ_{dc} value of the $CaRuO_3$ film is larger than its bulk value by a factor of 3, due to the strain effect.

To obtain optical properties of the (Ca,Sr)RuO_3 films accurately in a wide frequency region of 0.23–5.0 eV, we combined reflectance and transmittance measurements with spectroscopic ellipsometry [20]. Between 0.23 and 3.0 eV, $\sigma_1(\omega)$ were obtained accurately from reflectance and transmittance spectra using the Fresnel equations. Above 1.5 eV, $\sigma_1(\omega)$ were determined by spectroscopic ellipsometry. In these methods, any extrapolation procedures, which are commonly used in the Kramers-Kronig analysis of reflectance spectra [21], were not required.

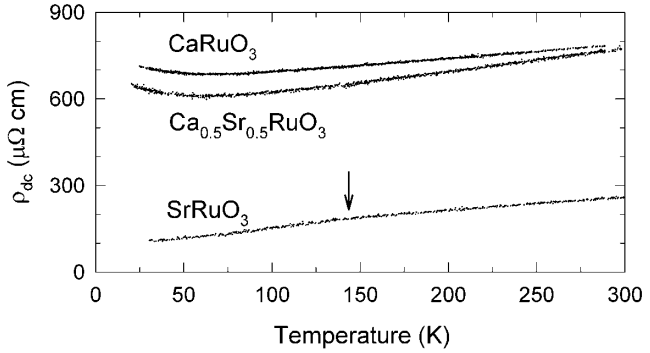

FIG. 2. Resistivity versus temperature for (Ca,Sr)RuO_3. Arrow indicates the Curie temperature of $SrRuO_3$.

Figure 3(a) shows $\sigma_1(\omega)$ of the (Ca,Sr)RuO_3 films. Below $\sim$1 eV, we can see the QP peaks whose dc limits agree with the measured dc conductivity values, marked with symbols. As Ca replaces Sr, the QP peak decreases. In the frequency region of 1–2 eV, there are broad features of the $U/2$ peaks. Around 3 eV, the U peaks can be seen with a very broad background absorption [22]. The background comes from the charge transfer excitation between O($2p$) and Ru($4d$) whose peak energy is higher than U [23]. Its estimated contribution is indicated with the dash–double-dotted line. Even with this charge transfer contribution, the spectral feature in Fig. 3(a) resembles Fig. 1(b) quite closely.

Figure 3(b) shows $\sigma_1(\omega)$ after the background absorption is subtracted. Note that the QP peaks are not changed very much after the subtraction. From these spectra, U_m and W_m are experimentally determined from the center and the half-width of the U peak [24]: values of $\{U_m, W_m\}$, in units of eV, are $\{2.99 \pm 0.05, 1.16 \pm 0.07\}$ for $CaRuO_3$, $\{3.07 \pm 0.05, 1.20 \pm 0.04\}$ for $Ca_{0.5}Sr_{0.5}RuO_3$, and $\{3.23 \pm 0.05, 1.31 \pm 0.04\}$ for $SrRuO_3$. As Sr replaces Ca, the relative increase in W_m is larger than that of U_m. Therefore, *the (Ca,Sr)RuO_3 films can be considered effective as a bandwidth controlled Mott-Hubbard system.*

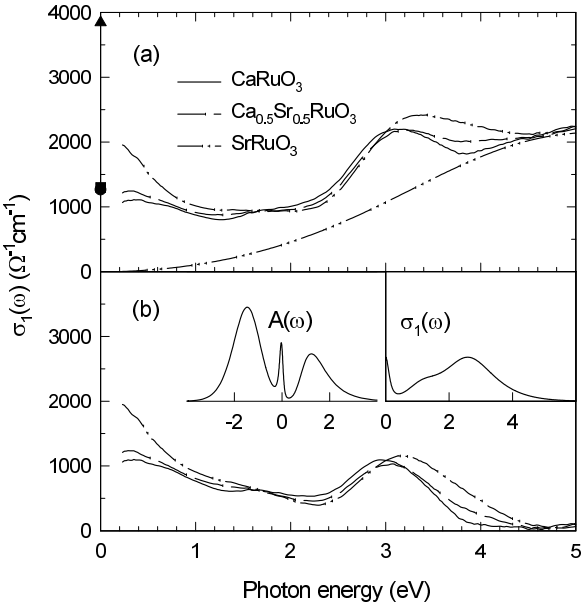

FIG. 3. (a) Optical conductivity spectra of (Ca,Sr)RuO_3 films at room temperature. Symbols indicate dc values obtained from dc measurements (▲: $SrRuO_3$; ■: $Ca_{0.5}Sr_{0.5}RuO_3$; and •: $CaRuO_3$). Dash–double-dotted line shows the charge transfer transition between O($2p$) and Ru($4d$) [23]. (b) Optical conductivity spectra after the charge transfer transition contribution is subtracted. Inset: single particle spectral function and optical conductivity calculated from a QMC simulation of DMFT with $U/W \sim 1.95$ for the 4/6-filled triple degenerate orbitals.

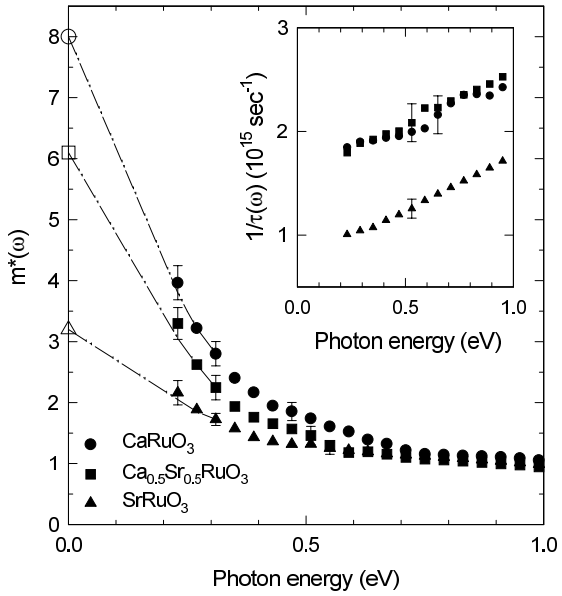

FIG. 4. Low energy mass enhancement $m^*(\omega)$ obtained from optical data using the extended Drude model. m^*'s from specific heat measurements are shown with ○ ($CaRuO_3$), □ ($Ca_{0.5}Sr_{0.5}RuO_3$), and △ ($SrRuO_3$) [16,18]. The dash-dotted lines are guidelines for the eye. The inset shows the corresponding frequency dependent scattering rate, $1/\tau(\omega)$.

The broad feature of the QP peaks could be described with the extended Drude model [25], which provides information on frequency dependent mass $m^*(\omega)$ and scattering rate $1/\tau(\omega)$ [26]. As shown in Fig. 4, all of the samples showed mass enhancements as frequency becomes lowered. Values of $m^*(\omega = 0)$, i.e., m^*, determined by specific heat measurements are marked with open symbols [16,18]. Since the carrier concentration is fixed for the (Ca,Sr)RuO_3 films, the enhancement of m^* could be attributed to the correlation effect. As Ca replaces Sr, m^* becomes larger [27], indicating that the $CaRuO_3$ is closer to the Mott M-I transition due to band narrowing. The inset in Fig. 4 shows spectra of $1/\tau(\omega)$ for our (Ca,Sr)RuO_3 films. Its frequency dependence is almost linear up to 1 eV and the slopes are nearly the same for all samples. This linear frequency dependence has been observed in many other correlated systems [10,11,28]; however, there is still no concrete explanation for this behavior.

It is not easy to understand the linear $1/\tau(\omega)$ with either GBR or DMFT, because both of them predict a Fermi liquidlike scattering, i.e., ω^2 dependency and accordingly frequency independent $m^*(\omega)$. If $1/\tau(\omega)$ is linear in ω, $m^*(\omega)$ should increase as $-\ln(\omega/\omega_0)$ by causality. And the critical energy scale ω_0 is related most probably to those of extra unusual scatterings (for example, local magnetic fluctuations), which might be beyond the Fermi liquid description and whose interplays with correlation effects are not fully understood yet. Anyway, the frequency dependence shown in Fig. 4 undoubtedly testifies an existence of such extra scattering mechanisms besides the Mott-Hubbard correlation effects.

Within the GBR picture for the Mott transition, the spectral weight of the QP peak, ω_p^{*2}, is an order parameter and should be proportional to $1/m^*$. Using a relation such that

$$\omega_p^{*2} \simeq 8 \int_0^{1\,\mathrm{eV}} \sigma_1(\omega) d\omega \,, \qquad (2)$$

ω_p^{*2} values for the (Ca,Sr)RuO_3 films could be estimated. As shown in Fig. 5(a), the measured values of ω_p^{*2} are quite linear to $1/m^*(\omega = 0.23\ \mathrm{eV})$ with a very small y-axis intercept, which demonstrates that most of the free carriers in the (Ca,Sr)RuO_3 films behave like correlated QP's in the Mott picture even though extra scattering mechanisms seem to be important.

Figure 5(b) shows the dependence of $(U/W)^2$ on $1/m^*$. $(U_m/W_m)^2$ shows linear behavior with respect to $(-1/m^*)$ but does not extend to zero when m^* goes to unity, which is not fully compatible with Eq. (1). One possibility is that the way to determine the value of U_m experimentally from the U peak position might overestimate the actual U value, which is due to the "band repulsion" effect [10]. To see this effect more clearly, we have performed quantum Monte Carlo (QMC) for the case of 4/6 filling of the triple degenerate Hubbard model in infinite dimensions. Compared to the nondegenerate 1/2 filled case, $(U/W)_c$ becomes larger, i.e., 2.0 [29]. And, in the metallic side near the M-I transition, the position of the U peak is located at a higher energy than the actual value of U, as shown in the inset in Fig. 3(b).

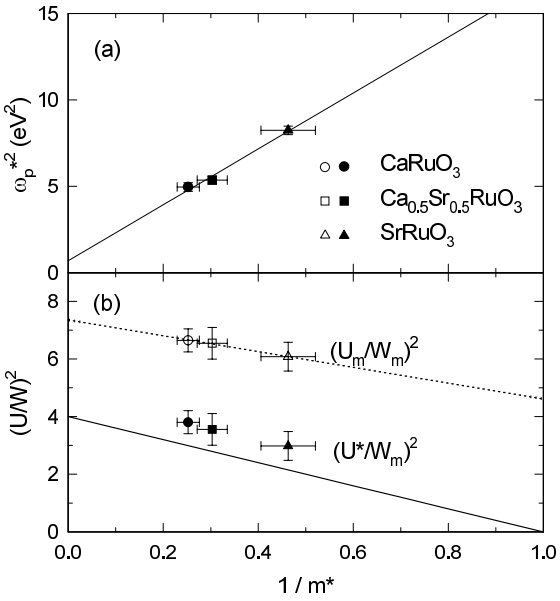

FIG. 5. (a) Spectral weight of the QP peak, ω_p^{*2}, versus $1/m^*$. (b) $(U/W)^2$ versus $1/m^*$. Two cases with different U values are shown, i.e., U_m (measured from the U peak) and U^* (~2.26 eV from QMC) are used. The solid line in (b) follows Eq. (1) with $(U/W)_c = 2.0$ for the 4/6-filled triple degeneracy.

The QMC result with $U/W \sim 1.95$ provides an overall good fit to $CaRuO_3$ data in terms of energy scales and main spectral structures. With this value of $U/W \sim 1.95$ from QMC and W_m, we estimated that the actual U value for $CaRuO_3$ should be around 2.26 eV. Assuming that this QMC-estimated value of U, U^* is the same for other ruthenate films, we plot $(U^*/W_m)^2$, which shows a much better agreement with the GBR picture, i.e., Eq. (1) with $(U/W)_c = 2.0$.

The QMC result, displayed in the inset in Fig. 3(b), shows that the predicted QP peak width is much narrower than the measured value, but it is a well-known shortcoming of DMFT. More theoretical considerations are required to explain the broad QP peak, which might relate with the extra scattering mechanisms indicated by the linear frequency dependence. Moreover, other factors, such as p-d hybridization, might be important for $(Ca,Sr)RuO_3$. Further investigations on the interplay of such interactions with Mott-Hubbard physics might provide us some more insight in $4d$ electrons of ruthenates.

In summary, we found that $(Ca,Sr)RuO_3$ is a $4d$ metal compound which has strong electron correlation effects. Its optical spectra display the spectral characteristics predicted for a metallic Mott-Hubbard system. However, low frequency behaviors of electrodynamic quantities indicate the existence of extra scattering mechanisms, which are beyond the correlated Fermi liquid description with either GBR or DMFT.

This work was supported by the Ministry of Education through BSRI-97-2416 and by the Korea Science and Engineering Foundation (KOSEF) through the RCDAMP of Pusan National University.

[1] N. F. Mott, *Metal-Insulator Transitions* (Taylor & Francis, London, 1990), 2nd ed.; *Metal-Insulator Transitions Revisited,* edited by P. P. Edwards and C. N. R. Rao (Taylor & Francis, London, 1995); A. Husmann, D. S. Jin, Y. V. Zastavker, T. F. Rosenbaum, X. Yao, and J. M. Honig, Science **274**, 1874 (1996).

[2] A. Georges, G. Kotliar, W. Krauth, and M. J. Rozenberg, Rev. Mod. Phys. **68**, 13 (1996), and references therein.

[3] W. F. Brinkman and T. M. Rice, Phys. Rev. B **2**, 4302 (1970).

[4] m^* is a normalized quantity with respect to band mass for an uncorrelated system.

[5] T. Arima, Y. Tokura, and J. B. Torrance, Phys. Rev. B **48**, 17006 (1993).

[6] Y. Tokura *et al.,* Phys. Rev. Lett. **70**, 2126 (1993); T. Katsufuji, Y. Okimoto, and Y. Tokura, Phys. Rev. Lett. **75**, 3497 (1995).

[7] Y. Okimoto, T. Katsufuji, Y. Okada, T. Arima, and Y. Tokura, Phys. Rev. B **51**, 9581 (1995).

[8] M. J. Rozenberg, I. H. Inoue, H. Makino, F. Iga, and Y. Nishihara, Phys. Rev. Lett. **76**, 4781 (1996).

[9] M. J. Rozenberg *et al.,* Phys. Rev. Lett. **75**, 105 (1995).

[10] H. Makino, I. H. Inoue, M. J. Rozenberg, I. Hase, Y. Aiura, and S. Onari, Phys. Rev. B **58**, 4384 (1998).

[11] I. H. Inoue *et al.,* Phys. Rev. Lett. **74**, 2539 (1995).

[12] Y. Maeno *et al.,* Nature (London) **372**, 532 (1995).

[13] T. Yokoya, A. Chainani, T. Takahashi, H. Katayama-Yoshida, M. Kasai, and Y. Tokura, Phys. Rev. Lett. **76**, 3009 (1996).

[14] T. Katsufuji, M. Kasai, and Y. Tokura, Phys. Rev. Lett. **76**, 126 (1996).

[15] G. Cao, S. McCall, J. E. Crow, and R. P. Guertin, Phys. Rev. Lett. **78**, 1751 (1997).

[16] G. Cao, S. McCall, M. Shepard, J. E. Crow, and R. P. Guertin, Phys. Rev. B **56**, 321 (1997).

[17] P. Kostic *et al.,* Phys. Rev. Lett. **81**, 2498 (1998).

[18] P. A. Cox, R. G. Egdell, J. B. Goodenough, A. Hamnett, and C. C. Naish, J. Phys. C **16**, 6221 (1983).

[19] R. A. Rao *et al.,* Appl. Phys. Lett. **70**, 3035 (1997); C. B. Eom *et al.,* Science **258**, 1766 (1992).

[20] H. S. Choi, J. Bak, J. S. Ahn, N. J. Hur, T. W. Noh, and J. H. Cho, J. Korean Phys. Soc. **33**, 185 (1998).

[21] K. H. Kim, J. H. Jung, and T. W. Noh, Phys. Rev. Lett. **81**, 1517 (1998).

[22] $U \sim 3$ eV is reported from photoelectron studies of $SrRuO_3$; see K. Fujioka *et al.,* Phys. Rev. B **56**, 6380 (1997).

[23] From previous results [18,22], we estimated the charge transfer excitation between $O(2p)$ and $Ru(4d)$ as a single Lorentzian peak, whose center and width are 5 and 6 eV, respectively.

[24] For experimental determination, see also G. A. Thomas *et al.,* Phys. Rev. Lett. **73**, 1529 (1994); Ref. [9]; and Fig. 62 of Ref. [2].

[25] J. W. Allen and J. C. Mikkelsen, Phys. Rev. B **15**, 2952 (1977); B. C. Webb, A. J. Sievers, and T. Mihalisin, Phys. Rev. Lett. **57**, 1951 (1986).

[26] For the calculation, plasma frequency $\omega_p = 3.9$ eV is used.

[27] m^* reported for $Ca_{0.25}Sr_{0.75}RuO_3$ and $Ca_{0.75}Sr_{0.25}RuO_3$ [16] were not monotonic along with the other data, and electron correlation alone cannot explain such deviations.

[28] Z. Schlesinger *et al.,* Phys. Rev. Lett. **65**, 801 (1990).

[29] From our QMC simulation, $(U/W)_c \simeq 2.3$ for half filling, 2.0 for 2/6 and 4/6 fillings, and 1.9 for 1/6 and 5/6 fillings for the triple degenerate case. For the calculation, we used the DMFT with $T = 1/12$ (in the unit of $W/2 = 1$).